ISSN 0020-1685, Inorganic Materials, 2007, Vol. 43, No. 8, pp. 901–909. © Pleiades Publishing, Inc., 2007.
Original Russian Text © T.V. Safronova, M.A. Shekhirev, V.I. Putlyaev, Yu.D. Tret'yakov, 2007, published in Neorganicheskie Materialy, 2007, Vol. 43, No. 8, pp. 1005–1014.

Hydroxyapatite-Based Ceramic Materials Prepared Using Solutions of Different Concentrations

T. V. Safronova, M. A. Shekhirev, V. I. Putlyaev, and Yu. D. Tret'yakov

Moscow State University, Vorob'evy gory 1, Moscow, 119899 Russia

e-mail: safronova@inorg.chem.msu.ru

Received October 11, 2006

Abstract—Hydroxyapatite, $Ca_{10}(PO_4)_6(OH)_2$, powders with enhanced sinterability have been synthesized through precipitation from calcium nitrate and ammonium hydrogen phosphate solutions at pH 9, $t = 60°C$, and a Ca/P atomic ratio of 1.67, and their properties have been studied: phase composition, particle size distribution, loose density, and green density. The initial solution concentration is shown to influence the properties of the powders and the ceramics fabricated from them. Comparison of the particle size distributions in disaggregated powders and the grain size distributions in the ceramics indicates that the ceramics inherit the structure of the corresponding powders. Optimizing the synthesis conditions in order to enhance the sinterability of the powders, we obtained green compacts with the highest shrinkage rate in the range 850–950°C and shrinkage onset at 600°C, which is 100–150°C lower in comparison with powders synthesized in earlier studies from calcium nitrate and ammonium hydrogen phosphate.

DOI: 10.1134/S0020168507080158

INTRODUCTION

The engineering of biomaterials for bone substitution is a promising area of research, which has seen rapid progress in recent years. Bone tissue is a composite material with a multilevel structural hierarchy, based on ultrafine-particle carbonate hydroxyapatite ($Ca_{10-x-y/2}(HPO_4)_x(CO_3)_y(PO_4)_{6-x-y}(OH)_{2-x}$) and collagen [1].

Currently, one of the challenges in medical materials research is to create materials well-suited for advanced maxillofacial reconstruction techniques [2]. Calcium phosphates, in particular hydroxyapatite (HA), $Ca_{10}(PO_4)_6(OH)_2$, are very similar in chemical composition to bone tissue. For this reason, the most widely used bone implant materials are dense or porous HA-based ceramics [3].

As in the case of many other ceramic materials, the fabrication of ceramics from powder HA involves the following steps: powder synthesis, forming, drying, and firing of dried bodies. The ceramics thus produced retain the key structural features of the starting powder. Consequently, the first process step is of prime importance since it determines the structural perfection of the powder and, hence, the microstructure and properties of the ceramic [4].

The processes for the preparation of calcium phosphate powders can be divided into two groups:

wet synthesis, which involves reactions between starting chemicals in solution or suspension, and

solid-state synthesis [5].

Solid-state reactions are commonly run at high temperatures, which inevitably increases the particle size of the resulting powder, reduces its specific surface area, and improves its structural perfection, thereby impairing the sinterability of the powder [6]. Moreover, solid-state synthesis does not always ensure sufficient homogeneity of the powder in chemical and phase compositions [7]. Wet-chemical processes are essentially free of these drawbacks and are better suited to the preparation of powders appropriate for the fabrication of ceramics with homogeneous polycrystalline microstructures.

The preparation of HA powders, including ceramic powders, involves the following steps: solution preparation, coprecipitation, aging of the precipitate, separation of the precipitate from the mother solution, washing of the precipitate, drying at 80–100°C, and calcination of the powder at 700–800°C [8, 9].

HA is most frequently synthesized by reacting calcium nitrate and ammonium phosphate or calcium hydroxide and phosphoric acid [10, 11]. The important advantage of the former reaction is that the Ca/P ratio can be maintained at 1.67 with high accuracy. Moreover, the reaction byproduct is ammonium nitrate, NH_4NO_3. Owing to its high solubility, ammonium nitrate remains, for the most part, in solution. NH_4NO_3 fully decomposes at relatively low temperatures and is thought to have an insignificant effect on the sintering behavior of the HA powder. For this reason, a number of investigators believe that the HA powders synthesized in this way can be sintered without removing the byproduct by washing [12].

Table 1. Initial Ca^{2+} and HPO_4^{2-} molar concentrations in solutions

No.	$[Ca^{2+}]/[HPO_4^{2-}]$
1	1.3/1
2	1/0.6
3	0.5/0.3
4	0.25/0.15

Powders precipitated from solutions consist of very fine (≤100 nm) particles and, hence, have a large surface energy. The powders tend to reduce it through spontaneous aggregation, during both synthesis and subsequent processing (drying, heat treatment). For this reason, the powder must be disaggregated, preferably in a low-boiling liquid [13].

As pointed out by Liu et al. [14], the solution temperature during HA precipitation has a significant effect on the crystallization kinetics of the precipitating amorphous calcium phosphate. In particular, full conversion of amorphous calcium phosphate to HA at 60°C takes 5 min. Synthesis at elevated temperatures (e.g., at 90°C), as well as aging [15], improves the structural perfection of the material, i.e., reduces the defect density in the crystallites constituting its particles, and, therefore, impairs the sintering behavior of the synthesized powder. These observations suggest that the aging step, which is sometimes conducted for several weeks or months [16], should be excluded from the preparation of ceramic HA powder, or its duration should be limited to several minutes.

According to previous work [17, 18], x-ray phase-pure HA can only be obtained by heat treatment at 700–800°C. For this reason, the preparation of HA powder often includes heat treatment at these temperatures. The fabrication of HA-based ceramic materials must include firing at temperatures no lower than 1000°C. Maintaining the key synthesis parameters (pH and Ca/P ratio) at the optimal level ensures the formation of crystalline apatite. Note that preliminary heat treatment at 700–800°C dramatically reduces the sinterability of the powder, which may have an adverse effect on the microstructure of the resultant ceramic. Therefore, such processing of HA powders appears unreasonable.

HA powders suitable for ceramic fabrication must meet a number of requirements:

(1) The Ca/P ratio must be 1.67.

(2) The phase composition of the powder must ensure the desired phase composition of the ceramic.

(3) The powder must consist of fine particles and, hence, have a large specific surface area.

(4) It must have a certain structural organization (e.g., a certain relationship between aggregates of different sizes).

(5) The crystallites constituting powder particles must have a highly imperfect structure.

The last three requirements pertain directly to sinterability, an important qualitative characteristic of ceramic powders. High sinterability makes it possible to reduce the firing temperature and duration. A small particle size and narrow aggregate size distribution in the starting powder offer the possibility of fabricating ceramics with a homogeneous, fine microstructure.

Control over the ceramic microstructure is possible, and often very effective, even in the powder synthesis step [19]. One possible way of controlling the ceramic microstructure is by varying the concentrations of raw materials in solution. Nevertheless, there is extremely limited information concerning the influence of reactant concentrations in solution on the properties of HA powders (composition, particle size, rheological behavior, sinterability) and ceramic microstructure.

The purpose of this work was to study the effect of synthesis conditions (reactant concentrations) on the properties of HA powders and ceramics.

EXPERIMENTAL

HA was synthesized by the reaction

$$10Ca(NO_3)_2 + 6(NH_4)_2HPO_4 + 8NH_4OH = Ca_{10}(PO_4)_6(OH)_2\downarrow + 20NH_4NO_3 + 6H_2O. \quad (1)$$

An $(NH_4)_2HPO_4$ solution (1.3, 1, 0.5, or 0.25 M) was added dropwise to a $Ca(NO_3)_2$ solution (1, 0.6, 0.3, or 0.15 M) at a rate of 3.5 ml/min. The reaction was run at 60°C with vigorous stirring. The solution was adjusted to pH 9 with 25% aqueous ammonia. After aging for 30 min, the precipitate was collected on filter paper. The filtrate was dried in thin layers at room temperature for 48 h. The dried precipitate was disaggregated by grinding with acetone in a ball mill at an acetone : powder : ball weight ratio of 1 : 1 : 3. Next, the powder was dried at room temperature for 2 h, run through a 200-μm sieve, and then pressed at 50 or 100 MPa into bars $3 \times 6 \times 40$ mm in dimensions (1.3–1.5 g) on a PG-10 hydraulic press. The green compacts were fired at 1200°C for 6 h (heating rate of 5°C/min). To preclude the possible adverse effect of active ammonium nitrate decomposition in the first firing step, the conditions were adjusted so as to ensure slow decomposition of the byproduct. To this end, below 400°C the green compacts were heated at a rate of 1°C/min.

Thus, we investigated HA powders prepared at different solution concentrations and pressed HA samples (Table 1).

The densities of green compacts and ceramics were determined by mass and dimensions. X-ray diffraction (XRD) measurements were performed on a DRON-3M powder diffractometer (CuK_α or CoK_α radiation). The phases present were identified using ICDD PDF-4 data. The mean particle size was evaluated from XRD peak

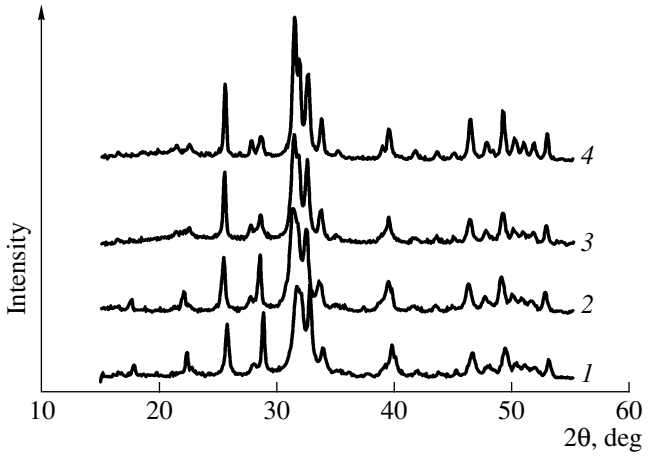

Fig. 1. XRD patterns of HA powders prepared from solutions with different concentrations: $[Ca^{2+}]/[HPO_4^{2-}]$ = (*1*) 1.3/1, (*2*) 1/0.6, (*3*) 0.5/0.3, (*4*) 0.25/0.15.

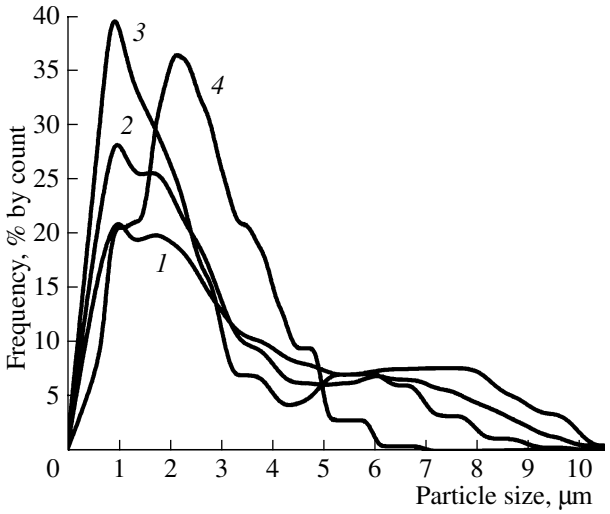

Fig. 2. Particle size distributions in HA powders prepared from solutions with different concentrations: $[Ca^{2+}]/[HPO_4^{2-}]$ = (*1*) 1.3/1, (*2*) 1/0.6, (*3*) 0.5/0.3, (*4*) 0.25/0.15.

widths using the Scherrer formula. To determine the intrinsic broadening of the 002 line (d = 3.44 Å), its shape was approximated by a Gaussian.

IR spectra were recorded on a Perkin-Elmer PE-1600 FTIR spectrophotometer from 400 to 4000 cm^{-1} with a 4-cm^{-1} step. Thermogravimetric (TG) analysis was performed in air during heating to 1000°C at a rate of 5°C/min, using a Perkin-Elmer Diamond Pyris analyzer.

Microstructures were examined by scanning electron microscopy (SEM) on a Carl Zeiss LEO Supra 50 VP (accelerating voltage, 5–10 kV) and by transmission electron microscopy (TEM) on a JEOL JEM-2000 FXII (accelerating voltage, 200 kV). Grain size distributions were extracted from SEM data in semiautomatic mode, using AnalySIS software. In microstructural analysis, we used four to seven micrographs from different sample areas. Distribution curves were obtained using data for 900 to 1300 grains.

The particle size distributions for powder samples were determined by laser diffraction in an aqueous medium using a Fritsch Analysette-22 instrument. Dilatometric data were obtained during heating to 1000°C at a rate of 5°C/min using a dilatometer equipped with a LIR-1400 optical displacement recorder.

RESULTS AND DISCUSSION

Preparation and properties of HA powders. XRD characterization showed that only two phases were present in our powders: HA and NH_4NO_3 (Fig. 1). The mean particle size of HA, evaluated from the width of the 002 XRD peak using the Scherrer formula, was found to increase systematically, from 20 to 45 nm, with decreasing solution concentration (with decreasing supersaturation with respect to HA). Similar results were obtained by TEM.

The particle size distributions extracted from laser diffraction data are displayed in Fig. 2. Characteristically, the primary particles in the powders synthesized by reaction (1) are severely aggregated, as evidenced by the significant asymmetry of the distribution curves, with extended "tails" at large particle sizes. Powders *1–3* ($[Ca^{2+}]/[HPO_4^{2-}]$ = 1.3/1, 1/0.6, and 0.5/0.3) have similar, bimodal distributions, in which one maximum is due to primary aggregates (~1–2 μm), and the other is due to secondary aggregates (~6–8 μm). The mean particle size is 4.15 μm in powder *1*, 3.36 μm in powder *2*, 2.73 μm in powder *3*, and 2.68 μm in powder *4*. The maximum size of the aggregates is within 11 μm. The fraction of secondary aggregates has a pronounced tendency to increase with increasing solution concentration (with decreasing crystallite size). At first glance, powder *4*, prepared using a dilute solution, differs in structural organization from the other powders. One possible reason for this is the weak interaction between coarse crystallites in aggregates, so that sonication, usually preceding laser diffraction measurements, readily breaks down large aggregates.

The rheological properties of powders depend on the size, shape, and surface morphology of the particles (aggregates). Moreover, isometric particles with a broad (or multimodal) size distribution are known to be more densely packed in powders and green compacts (the highest density can be achieved at a certain relationship between size fractions) [20]. At $[Ca^{2+}]/[HPO_4^{2-}]$ = 1.3/1, 1/0.6, and 0.5/0.3, the percent-

Table 2. Densities (relative to HA, $d = 3.16$ g/cm^3) of HA powders, green compacts, and sintered materials

No.	Loose density, %	Green density, %		Density after firing, %	
		50 MPa	100 MPa	400°C*	1200°C
1	13	46	60	34	82
2	13	42	59	43	88
3	11	40	50	44	92
4	9	39	47	44	94

* Compaction at 50 MPa.

age of large aggregates was found to increase with solution concentration, which was accompanied by an increase in loose and green densities (Table 2). In addition, the presence of impurities (surfactants and reaction byproducts) may also have a significant effect on the rheological properties of the powders. In our samples, an increase in the content of ammonium nitrate captured by HA powder from the solution (i.e., an increase in solution concentration) is accompanied by an increase in loose and green densities. It seems likely that ammonium nitrate, like many ionic crystals with a low lattice energy, has a low yield stress and acts as a plasticizer, imparting plasticity to the powder system and reducing the interparticle friction.

The data in Table 2 demonstrates that increasing the compaction pressure from 50 to 100 MPa increases the green density, but the above-mentioned tendency of the green density to increase with an increase in the fraction of secondary aggregates persists. This leads us to assume that the qualitative picture of structural organization does not change drastically in going from the powders to the green compacts, even though the forming process reduces the size of secondary aggregates.

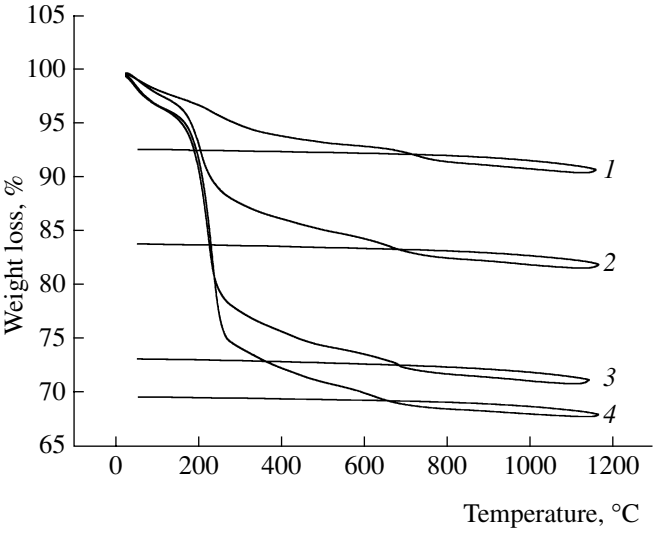

Fig. 3. TG curves of HA powders prepared from solutions with different concentrations: $[Ca^{2+}]/[HPO_4^{2-}]$ = (*1*) 1.3/1 and 0.25/0.15, (*2*) 0.5/0.3, (*3*) 1/0.6, (*4*) 1.3/1.

Thus, the structural organization of the HA powders can be represented by the following model: dense primary aggregates 1–2 μm in size form looser aggregates on the order of 8 μm in size; the density of the secondary aggregates and the interparticle forces in them decrease with decreasing initial salt concentration in the solution.

Thermal behavior of the powders. TG data demonstrate that, on heating to 1150°C, the HA powders experience a significant weight loss, up to 30% at the highest solution concentration. The TG curves show two steps of weight loss (Fig. 3). The first step (below ~5–6%) is attributable to the removal of water and acetone (disaggregation medium). The second step (200–700°C, ~25%) seems to be due to ammonium nitrate decomposition by the reaction

$$NH_4NO_3 = N_2O\uparrow + 2H_2O\uparrow \quad (2)$$

and to the removal of chemisorbed water. The decomposition rate reaches a maximum at 250°C.

Since the powders were synthesized in air, CO_2 capture by the alkali solution and CO_3^{2-} incorporation into the HA structure were unavoidable. Therefore, the weight loss at temperatures below 850–900°C is attributable to carbonate hydroxyapatite decomposition and CO_2 release [21]. After the removal of all the carbonate groups, the weight loss is associated with partial HA dehydration, which is reversible, as evidenced by the weight gain during cooling (Fig. 3), and leads to the formation of oxyhydroxyapatite [1]:

$$Ca_{10}(PO_4)_6(OH)_2 \longrightarrow Ca_{10}(PO_4)_6(OH)_{2-2x}O_x + xH_2O\uparrow. \quad (3)$$

The thermal analysis data for our samples indicate that the weight loss increases with increasing solution concentration and, hence, with increasing ammonium nitrate content in the powders. The weight loss at 1150°C, contributed mainly by ammonium nitrate decomposition, as a function of solution concentration has a tendency to saturate (Fig. 4). It is reasonable to assume that the capture of the byproduct is associated with the adsorption of ions from the mother solution on

the surface of the HA precipitate. The curve in Fig. 4 then represents an adsorption isotherm because the fraction of the captured ammonium nitrate must be proportional to the amount of adsorption per gram of the adsorbent. It is well known [22] that positive deviations of the amount of adsorption from the solution composition attests to strong adsorption of the component (e.g., NH_4NO_3) compared to water. This is in conflict with the opinion often encountered in the literature that the NH_4^+ and NO_3^- ions do not participate in adsorption interactions and, hence, do not influence the shape and size of HA crystallites [23]. Moreover, in this study HA was synthesized at pH 9, i.e., under conditions close to the isoionic point of the HA surface (according to Chander and Fuerstenau [24], the HA surface is electrically neutral at pH 8.7), which prevented ion adsorption from solution. Therefore, only a small fraction of the ammonium nitrate was adsorbed by the powder. A significant fraction of this salt was captured by dense aggregates of HA crystallites (intercrystalline capture). In addition, the precipitating amorphous calcium phosphate has a mesoporous structure, with the pores filled by the mother solution. As shown by Tadic et al. [25], the HAP crystallizing from amorphous calcium phosphate during aging inherits its pore structure. This implies that some of the NH_4NO_3 may be present in primary HA crystallites as pore fluid.

According to IR spectroscopy data (Fig. 5), the powders heat-treated at 400°C contain residual carbonate groups and ammonium nitrate, a byproduct of reaction (1). Thus, in spite of the low decomposition temperature of ammonium nitrate (about 200°C), it persists in the powder even after heat treatment at 400°C. XRD data indicate that firing at 1200°C leads to the formation of phase-pure HA in all of our samples. This leads us to conclude that the HA precipitated from calcium nitrate and ammonium hydrogen phosphate solutions is stable and has the stoichiometric composition because even slight deviations from stoichiometry reduce the decomposition temperature of HA to 700°C [21].

Sintering behavior of HA powders. The dilatometric curves of our samples (Fig. 6) are similar in shape. The shrinkage rate reaches a maximum in the range 850–950°C. All of the curves have two characteristic portions. At temperatures from 150 to 250°C, shrinkage is driven by the capillary forces of the molten ammonium nitrate present in the pores of the material. In the range 700–950°C, the variation in sample dimensions is due to the elimination of pores and densification of the material, which corresponds to the initial stage sintering of HA. With increasing solution concentration (decreasing particle size), densification begins at lower temperatures and exhibits "smoother behavior," i.e., with decreasing solution concentration, densification occurs in a narrower temperature rage.

The SEM micrograph of a fracture surface of one of the samples heat-treated at 400°C (Fig. 7) demonstrates that, after heating, the material contains large aggregates. The nonuniform density distribution in the material is due to heat-treatment-induced aggregation. In addition to dense aggregates, the micrograph shows lower density zones and small cracks, which are likely to result from ammonium nitrate decomposition. Note that the minimum size of the dense zones is no greater than 1–2 μm, which corresponds to the size of the primary aggregates in the precipitated powders.

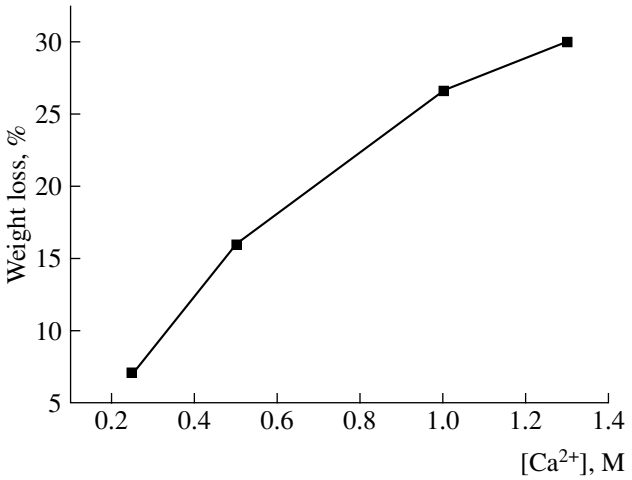

Fig. 4. Weight loss at 1150°C in HA powders prepared from solutions with different concentrations.

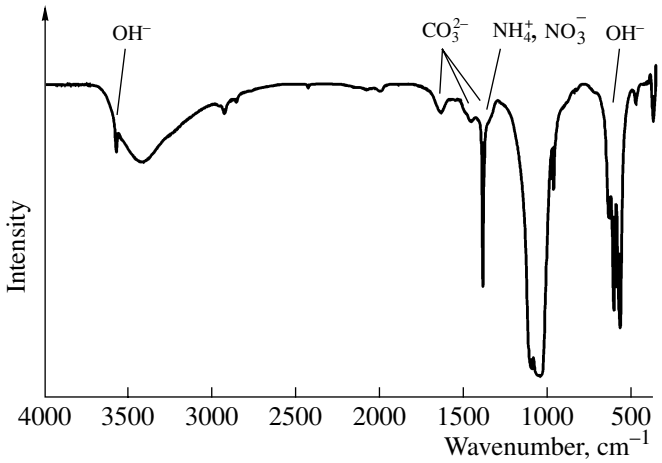

Fig. 5. IR spectrum of the HA powder synthesized at $[Ca^{2+}]/[HPO_4^{2-}] = 1/0.6$ and heat-treated at 400°C.

The densities of the HA powders, green compacts, and ceramics are listed in Table 2. The relative density of the green compacts increases with byproduct content. After firing at 400°C, the relative density of the samples is higher at lower byproduct contents, which implies that the byproduct acts as an inert burnable additive. Considering the relative densities of the samples heat-treated at 400°C as initial densities for the sin-

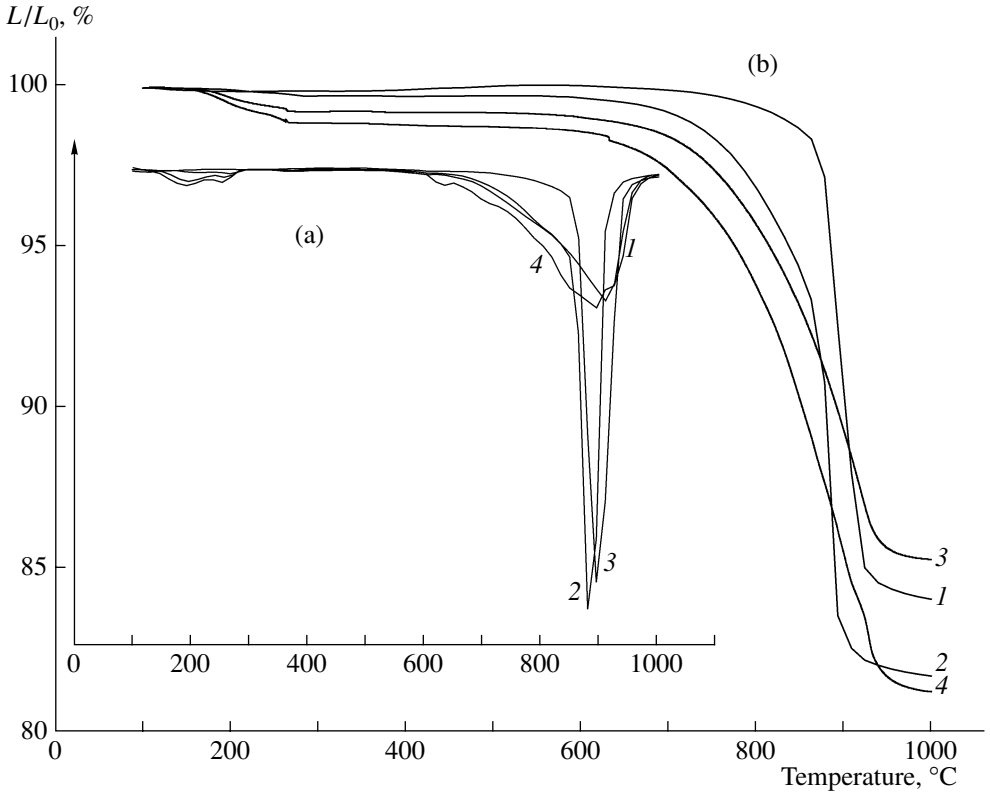

Fig. 6. (a) Differential and (b) integral dilatometric curves of HA powders prepared from solutions with different concentrations: $[Ca^{2+}]/[HPO_4^{2-}]$ = (*1*) 0.25/0.15, (*2*) 0.5/0.3, (*3*) 1/0.6, (*4*) 1.3/1.

tering process, we see that the densification of samples *3* and *4* begins from a denser state (44%) and that, after heat treatment, sintering of these samples ensures higher densities, 92 and 94%, respectively. The relative density of sample *1* (1.3/1) is 34% after firing at 400°C and 82% after sintering at 1200°C. The change in density upon sintering at 1200°C after firing at 400°C is the smallest (45%) in sample *2* (1/0.6). The density of the other samples changes by 48–50%. Thus, the density has a tendency to increase with decreasing solution concentration. At the same time, the above results indicate that the density of the green compacts containing no byproduct has a preferable effect on the final density of the ceramics. The highest density was achieved in samples *3* and *4*, prepared using solutions with $[Ca^{2+}]/[HPO_4^{2-}]$ = 0.5/0.3 and 0.25/0.15.

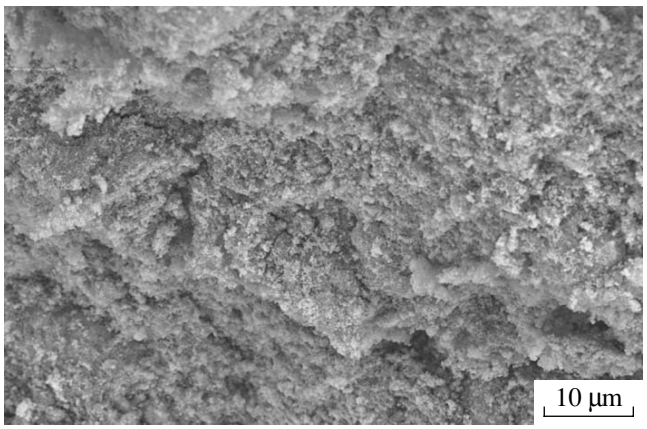

Fig. 7. SEM micrograph of a fracture surface of the HA sample prepared from the solution with $[Ca^{2+}]/[HPO_4^{2-}]$ = 1/0.6 and heat-treated at 400°C.

Thus, ammonium nitrate has different effects in different ceramic processing steps:

during compaction, it increases the green density;

during melting (170°C), it promotes densification;

during initial sintering (210–250°C) NH_4NO_3 decomposes, leading to N_2O release, which may break interparticle bonds in the sample; also possible is that NH_4NO_3 favors microexplosive disaggregation [26], thereby influencing the microstructural homogeneity of the material.

Given that ammonium nitrate has an ambiguous effect on the densification of HA powders and the properties of the resultant ceramics, it is necessary to optimize its content in the starting HA powder. In our opinion, optimization can be achieved either by adjusting the solution concentration or through controlled wash-

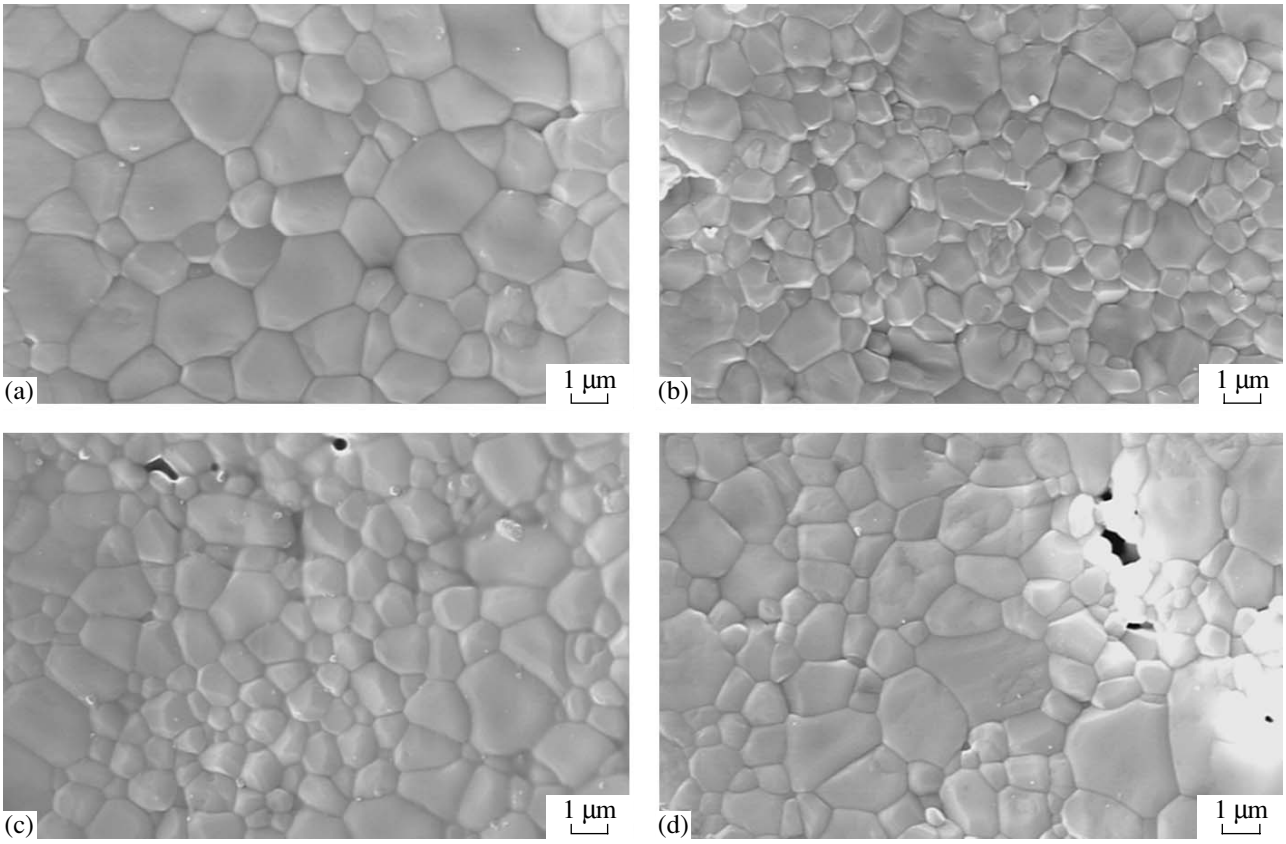

Fig. 8. SEM micrographs of fracture surfaces of HA ceramics prepared by sintering at 1200°C for 6 h: $[Ca^{2+}]/[HPO_4^{2-}]$ = (a) 0.25/0.15, (b) 0.5/0.3, (c) 1/0.6, (d) 1.3/1.

ing of the precipitate, by varying not only the number of washing cycles but also the characteristics, such as volume and temperature, of the washing liquid.

High density of ceramics does not reflect the entire range of the properties of the material and cannot be used as a criterion for microstructural quality. In particular, it is well known [27, 28] that the mechanical strength, a structure-sensitive property, increases with decreasing grain size.

Microstructural examination of the ceramics prepared by sintering at 1200°C for 6 h showed that the sample with $[Ca^{2+}]/[HPO_4^{2-}]$ = 0.25/0.15 was the most homogeneous. In addition, it had an increased grain size (Fig. 8), without intercrystalline pores. This indicates that pores are eliminated before grain growth. Thus, with the firing and sintering temperatures used, densification and grain growth occur in different processing steps, which is known to facilitate the fabrication of dense, fine-grained ceramics (see, e.g., [29]).

Figure 9 shows the grain size distribution in the sample with $[Ca^{2+}]/[HPO_4^{2-}]$ = 0.25/0.15, which has the form of a typical unimodal curve. Comparison of the grain size distributions in samples prepared from solutions with different concentrations indicates that samples *1–3* (1.3/1, 1/0.6, and 0.5/0.3) are similar in grain size distribution. Note that the grain size distribution in a given ceramic is similar to the particle size distribution in the powder from which the ceramic was prepared (Fig. 10). The particle size distributions in the powders with $[Ca^{2+}]/[HPO_4^{2-}]$ = 0.5/0.3, 1/0.6, and 1.3/1 and the grain size distributions in the corresponding ceramics have a maximum at ~1 μm. The particle size distribution in sample 4 (0.25/0.15) passes through a maximum at ~2.3 μm. The grain size distribution in the corresponding ceramic peaks at ~1.4 μm. Comparison of the particle and grain size distributions demonstrates that the ceramics inherit the structure of the corresponding powders. Thus, we are led to conclude that the initial solution concentration plays an important role in determining the ceramic microstructure.

Note that the grain size of HA ceramics is determined by the size of the primary aggregates in the corresponding powder. Given that the primary and secondary aggregates in the HA powders differ in density, this observation suggests the following mechanisms of HA sintering:

(1) There is strong interaction between large-angle grain boundaries and pores, which inhibits grain

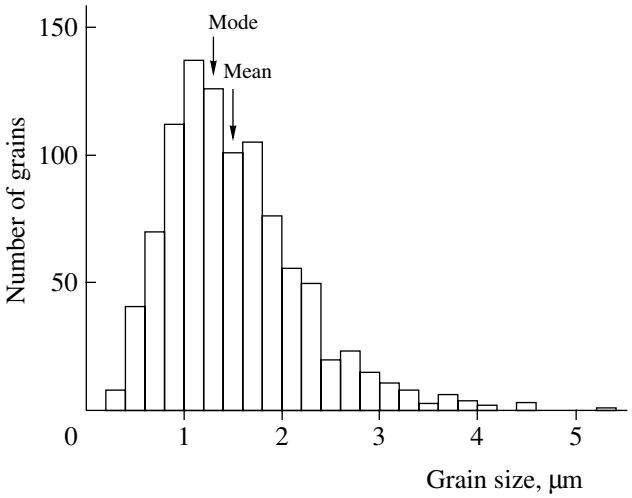

Fig. 9. Histogram of the grain size distribution in the ceramic prepared at $[Ca^{2+}]/[HPO_4^{2-}] = 0.25/0.15$.

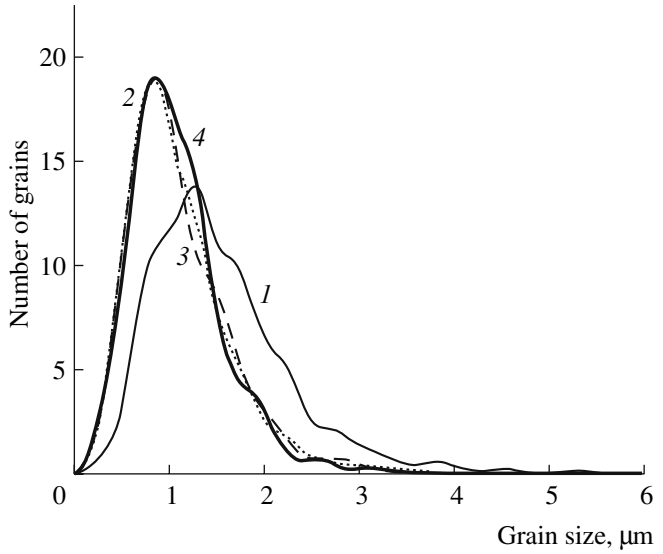

Fig. 10. Grain size distributions in the ceramics prepared at $[Ca^{2+}]/[HPO_4^{2-}]$ = (*1*) 1.3/1, (*2*) 1/0.6, (*3*) 0.5/0.3, and (*4*) 0.25/0.15.

growth. At the same time, the particles constituting a primary aggregate sinter rather rapidly to form a nucleus of a grain (to clarify this issue, additional TEM and dynamic light scattering studies of the structure of primary aggregates are needed.

(2) The high rate of pore elimination at rather low temperatures (according to dilatometry data, these temperatures are lower for smaller primary crystallites) indicates that surface processes play an important role in elementary sintering events, in agreement with earlier results [30]. It is, however, hardly appropriate to hold that surface diffusion or the vaporization–condensation process is the only mass transport mechanism because, otherwise, the observed significant volume shrinkage would be difficult to account for.

CONCLUSIONS

The present experimental data indicate that, in spite of its high solubility, ammonium nitrate is quantitatively captured by the precipitated HA. The amount of ammonium nitrate incorporated into the precipitate increases with solution concentration.

The high ammonium nitrate content (up to 30%) influences the rheological properties of the HA powders (densification and packing of the aggregates in the green compacts) and determines the behavior of the green bodies during heating to 250°C. During heat treatment in the range 160–200°C, ammonium nitrate promotes densification and rearrangement of HA particles in the molten salt owing to capillary forces. At the same time, after calcination at 400°C the sample density has another tendency and decreases with an increase in solution concentration and, hence, in the amount of adsorbed ammonium nitrate.

Thus, though identical in chemical composition, the powders differ in the initial conditions for densification during heat treatment and sintering. In the compacted powders with $[Ca^{2+}]/[HPO_4^{2-}] = 0.25/0.15$, which have the largest size of primary crystallites, the mass transport conditions are more favorable because of the higher initial density (at 400°C). In addition, the low loose density of these powders may be interpreted as evidence for a looser morphology of the aggregates of HA particles, which were formed under the least sterically hindered conditions. It is then reasonable to assume that the larger aggregates in the starting powder and the higher green density in comparison with the other samples are the major reason for the larger grain size and higher density of the corresponding ceramic.

Sintering of the HA prepared here begins at 600°C, that is, 100–150°C below the sintering temperature of powders synthesized in earlier studies by reacting calcium nitrate and ammonium hydrogen phosphate. The shrinkage rate of our samples reaches a maximum in the range 850–900°C. The density and microstructure of the ceramics depend significantly on synthesis conditions, in particular on the initial solution concentration. The grain size distribution in the ceramics correlates with the particle size distribution in the starting powders, which suggests that the ceramics inherit the structure of the corresponding powders.

ACKNOWLEDGMENTS

This work was supported by the Russian Foundation for Basic Research, grant nos. 05-03-32768-a and 06-08-01112.

REFERENCES

1. Hench, L.L., Bioceramics, *J. Am. Ceram. Soc.*, 1998, vol. 81, no. 7, pp. 1705–1728.
2. Sarkisov, P.D. and Mikhailenko, N.Yu., Bioactive Inorganic Materials for Bone Substitution, *Tekh. Tekhnol. Silikatov*, 1994, vol. 1, no. 2, pp. 5–11.
3. Putlyaev, V.I. and Safronova, T.V., Next-Generation Calcium Phosphate Biomaterials: The Role of Chemical and Phase Compositions, *Steklo Keram.*, 2006, no. 3, pp. 30–33.
4. Belyakov, A.V., Structure Evolution in Ceramic Processing, *Novye Ogneupory*, 2006, no. 1, pp. 56–61.
5. *Inorganic Phosphate Materials*, Kanazawa, T., Ed., Amsterdam: Elsevier, 1994.
6. Tret'yakov, Yu.D. and Putlyaev, V.I., *Vvedenie v khimiyu tverdofaznykh materialov* (Introduction to the Chemistry of Solids), Moscow: Mosk. Gos. Univ., 2006.
7. Barinov, S.M. and Komlev, V.S., *Biokeramika na osnove fosfatov kal'tsiya* (Calcium-Phosphate-Based Bioceramics), Moscow: Nauka, 2005.
8. Orlovskii, V.P., Kurdyumov, S.G., and Slivko, O.I., Synthesis, Properties, and Applications of Calcium Hydroxyapatite, *Stomatologiya*, 1996, vol. 75, no. 5, pp. 68–73.
9. Mal'kov, M.A., Lipochkin, S.V., Mosin, Yu.M., et al., Hydroxyapatite Ceramics for Medical Applications, *Steklo Keram.,* 1991, no. 7, pp. 28–29.
10. Veresov, A.G., Putlyaev, V.I., and Tret'yakov, Yu.D., Advances in Calcium Phosphate Biomaterials, *Ross. Khim. Zh.*, 2000, vol. 44, no. 6, part 2, pp. 32–46.
11. Melikhov, I.V., Komarov, V.V., Severin, A.V., et al., Two-Dimensional Crystalline Hydroxyapatite, *Dokl. Akad. Nauk*, 2000, vol. 373, no. 3, p. 355.
12. Raynaud, S., Champion, E., Bernache-Assollant, D., and Thomas, P., Calcium Phosphate Apatites with Variable Ca/P Atomic Ratio: I. Synthesis, Characterisation, and Thermal Stability of Powders, *Biomaterials*, 2002, vol. 23, pp. 1065–1072.
13. Balkevich, V.L., *Tekhnicheskaya keramika* (Technical Ceramics), Moscow: Stroiizdat, 1984.
14. Liu, C., Huang, Y., Shen, W., and Cui, J., Kinetics of Hydroxyapatite Precipitation at pH 10 to 11, *Biomaterials*, 2001, vol. 22, pp. 301–306.
15. Rodriguez-Lorenzo, L.M. and Vallet-Regi, M., Controlled Crystallization of Calcium Phosphate Apatites, *Chem. Mater.*, 2000, vol. 12, pp. 2460–2465.
16. Koutsopoulos, S., Synthesis and Characterization of Hydroxyapatite Crystals: A Review Study on the Analytical Methods, *J. Biomed. Mater. Res.*, 2002, vol. 62, pp. 600–612.
17. Klyuchnikov, N.G., *Rukovodstvo po neorganicheskomu sintezu* (Practical Guide to Inorganic Synthesis), Moscow: Khimiya, 1965.
18. Huber, V., Schmeiser, M., Schenk, V.P., et al., *Handbuch der präparativen anorganischen Chemie,* Stuttgart: Ferdinand Enke, 1978, 3rd ed.
19. Lukin, E.S., Advanced Dense Oxide Ceramics with Controlled Microstructure: Part I. Effect of Oxide Powder Aggregation on the Sintering and Microstructure of Ceramics, *Ogneupory Tekh. Keram.*, 1996, no. 1, pp. 5–14.
20. Andrianov, E.I., *Metody opredeleniya strukturno-mekhanicheskikh kharakteristik poroshkoobraznykh materialov* (Structural and Mechanical Characterization of Powder Materials), Moscow: Khimiya, 1982.
21. Vallet-Regi, M., Rodrigues-Lorenco, L.M., and Salinas, A.J., Synthesis and Characterization of Calcium Deficient Apatite, *Solid State Ionics*, 1997, vols. 101–103, pp. 1279–1285.
22. *Kurs fizicheskoi khimii* (Course in Physical Chemistry), Gerasimov, Ya.I., Ed., Moscow: Khimiya, 1970, vol. 1, pp. 496–503.
23. Stepuk, A.A. and Veresov, A.V., Effect of Precursor Anions (NO^{3-}, Cl^{-}, CH_3COO^{-}) and Heat Treatment on the Micromorphology of Hydroxyapatite: Potential Applications in Implants, *Materialy mezhdunarodnoi shkoly-konferentsii molodykh uchenykh* (Proc. Int. Workshop of Young Scientists), Tomsk, 2005, pp. 777–780.
24. Chander, S. and Fuerstenau, D.W., Interfacial Properties and Equilibria in the Apatite–Aqueous Solution System, *J. Colloid Interface Sci.*, 1979, vol. 70, no. 3, pp. 506–516.
25. Tadic, D., Veresov, A., Putlyaev, V.I., and Epple, M., In-Vitro Preparation of Nanocrystalline Calcium Phosphates as Bone Substitution Materials in Surgery, *Materialwiss. Werkstofftech.,* 2003, vol. 34, no. 12, pp. 1048–1051.
26. Sherif, F.G. and Via F.A., US Patent 4 764 357, 1988.
27. Kingery, W.D., *Introduction to Ceramics*, New York: Wiley, 1965.
28. *Khimicheskaya tekhnologiya keramiki* (Chemical Technology of Ceramics), Guzman, I.Ya., Ed., Moscow: Stroimaterialy, 2003, pp. 47–163.
29. Putlayev, V., Veresov, A., Pulkin, M., et al., Silicon-Substituted Hydroxyapatite Ceramics (Si-HAp): Densification and Grain Growth through the Prism of Sintering Theories, *Materialwiss. Werkstofftech.*, 2006, vol. 37, no. 6, pp. 416–421.
30. Bernache-Assollant, D., Ababou, A., Champion, E., and Heughebaert, M., Sintering of Calcium Phosphate Hydroxyapatite $Ca_{10}(PO_4)_6(OH)_2$: I. Calcination and Particle Growth, *J. Eur. Ceram. Soc.*, 2003, vol. 23, pp. 229–241.